

Comparative Study of Atomic and Electronic Structures of P and Bi Nanofilms

著者	Saito Mineo, Takemori Yohei, Hashi Tomofumi, Nagao Tadaaki, Yaginuma Shin
著者別表示	齋藤 峯雄
journal or publication title	Japanese Journal of Applied Physics
volume	46
number	12
page range	7824-7828
year	2007-12-06
URL	http://doi.org/10.24517/00065477

doi: <https://doi.org/10.1143/JJAP.46.7824>



Comparative study on the atomic and electronic structures of P and Bi nanofilms

Mineo Saito¹, Yohei Takemori¹, Tomofumi Hashi¹, Tadaaki Nagao^{2,3}, and Shin Yaginuma²

Division of Mathematical and Physical Science, Graduate School of Natural Science & Technology, Kanazawa University, Kakuma-machi, Kanazawa 920-1192, Japan¹
Institute for Materials Science, 1-2-1 Sengen, Tukuba, Ibaraki 305-8577, Japan²
ICORP, JST,4-1-8 Honcho,Kawaguchi,Saitama 332-0012, Japan³

(Received _____)

We perform first-principles calculations on P and Bi nanofilms and clarify the atomic and electronic structures of these films. The energy gap of the two-atomic layer film of P has the band gap of 1.2 eV, and as the thickness becomes large, the band gap becomes close to that of the bulk, which is a semiconductor. The most stable structure of the two-atomic-layer Bi film has the energy gap of 0.2 eV and two atoms on the surface are buckled. The nonbuckled structure is metallic and is metastable and its energy is slightly (12meV) higher than the buckled structure. We argue why the P films are nonbuckled and the stable Bi films are buckled.

KEYWORDS: metal, insulator, nanofilm, density functional theory

1. Introduction

It is well established that metals grow on semiconductor surfaces preferentially via the Stransky-Krastanov growth mode, i.e., due to stress energy relaxation, growth of three-dimensional islands follows the initial formation of the flat wetting layer.¹⁻³⁾ This growth mechanism is a severe drawback for achievement of flat well ordered films which are expected to be suitable for nano electronics applications. However, exceptional cases were reported.⁴⁻⁸⁾ For example, flat films of Pb and Ag on Si(111) surfaces were observed. Stable flat films having specific thicknesses, which are called magic thicknesses, contributes to this novel growth.⁹⁾ This stability of magic-thickness films observed at low temperatures was explained by an argument based on the quantum size effect, which originates from the electron confinement in the film-thickness direction. Very recently, the magic thicknesses were observed even at room temperature for Bi films on Si (111) surface,¹⁰⁾ i.e., the even-number atomic-layer-film is very stable. This novel stability of the flatness is found to be mainly due to the fact that the even-number-layer film takes the paired layer structure and is thus relatively less affected by the electron confinement.^{10,11)} By utilizing the novel flatness, Bi films are used as a template of the pentacene crystal,¹²⁾ so the films attract technologically interests.

In the initial stage of the Bi growth on Si(111) surface, rugged wetting layers are constructed on the Si(111) surface, then the crystalline Bi ultrathin films are grown. Since the Bi crystal forms arsenic structure, the film having a substantial thickness forms the arsenic structure. However, when the thickness is small, the film forms a different structure, i.e., the structure is similar to the black phosphorus structure, which is taken by P under the room temperature and ambient pressure. This peculiar structure of the Bi thin film is due to the fact that the surface energy of the black phosphorus structure is lower than that of arsenic structure.^{10,11)} It is well known that among the V elements, only P takes the black phosphorous structure while As, Sb, and Bi take arsenic structures. Then a question arises as to what is the structures of nanofilms of group V elements. To answer this question, we perform first-principles calculations on the atomic structures of P and Bi films and compare the atomic and electronic structures of these two kinds of

films.

2. Method

We perform density functional calculations within the generalized gradient approximation. The repeating slab model is used to simulate P and Bi films. The norm conserving pseudopotential is used for P and the cutoff energy of the plane wave basis set is taken to be 9Ry. For Bi, an ultrasoft pseudopotential and the plane wave basis set whose maximum kinetic energy is 12 Ry are used and the cut off energy for the charge mesh is taken to be 100 Ry. In the optimized geometry of the Bi crystal, the calculated lattice constants differ within 0.9% from the experimental values. The evaluation of the validity of our calculation on the P crystal is done in the next section. In the total energy calculations, the 6×6 mesh points are used as the sampling point in the two-dimensional Brillouin zone integration in the film calculations.

3. Results and discussion

We start from calculations on P crystal. In the optimized structure of the crystal(Fig. 1), the lengths of the a and c axes are 4.40 Å and 3.40 Å, respectively (Table I), which are close to the experimental values(4.39 Å and 3.31 Å).¹³⁾ The lattice length of the b axis in the stacking direction is 11.21 Å, which is slightly larger than the experimental value (10.48 Å). This difference is expected to originate from the fact that the density functional theory gives some error in the case of the van der Walls interaction. The calculated lengths of the horizontal bond(l_1) connecting the two top atoms is 2.27Å and that of the vertical bond connecting the top and second top atoms (l_2) is 2.29Å. The distance between the atoms in the neighboring layer is 3.88Å, which is much longer than the above horizontal and vertical bonds, corresponding to the fact that the layer interaction is of the van der Waals type. The calculated two bond angles, θ_1 and θ_2 are 97.2 ° and 103.7°, respectively. As shown in Table I, the calculated bond lengths and angles are close to the experimental values. The calculated bond angles(θ_1 and θ_2) are rather close to that of the sp^3 (109.5°) angle, which is due to the fact that P atom favors sp hybridization. As the total electron charge in Fig. 2(a) shows, each P atom has three chemical bonds and also has the dangling bond characterized by sp^3 hybridization. This dangling bond is due to the fact that the

P bond angles are close to the sp^3 bond angle.

We next perform calculations on 2, 4, and 6-layer films (The atomic configuration of the two-layer film is shown in Fig. 2(b)). We optimize the cell lengths and find that the lengths along the a-axes of the crystal are 4.64 Å, 4.61 Å, and 4.60 Å, respectively, for the 2, 4, and 6 layer films (Table I). The cell lengths of the c-axis are 3.37 Å, 3.38 Å and 3.38 Å, respectively. Therefore the length of the a-axis decreases and that of the c-axis increases as the layer thickness becomes large (Table I). However, the difference among the lattice constants of the three kinds of films is rather small and the values are close to those of crystals. This is due to the fact that the layer interaction is van der Waals type and is thus very weak. The density of states (DOS) of these films shown in Fig. 3 indicate that the band gap becomes small as the layer thickness becomes large. The band gaps of the two-layer, four-layer, and six-layer films are found to be 1.24 eV, 0.51 eV, and 0.49 eV, respectively. Experimental studies show that the P crystal is a semiconductor having the energy gap of 0.3 eV.¹⁴⁾ The above calculational results on P films suggest that the band gap decreases and becomes close to the crystal value as the thickness increases.

We now study the Bi film. When the film thickness is small, the black phosphorus type structure, which is different from the crystal one (arsenic structure) is known to be grown.¹⁰⁾ Here, we focus on the two-layer films and compare them with the P films. We find two optimized geometries (Fig. 4). In the most stable structure, the two top atoms are buckled and the amplitude of buckling is found to be 0.5 Å. In the metastable structure, the two atoms are nonbuckled and thus they are equivalent. The calculated DOS shown in Fig. 5 indicates that the most stable structure has the gap of 0.2 eV while the metastable structure has no band gap.

In the nonbuckled structure, the value of l_1 and l_2 are 3.06 Å and 2.97 Å, respectively. The bond angles θ_1 and θ_2 , respectively, are 95.9° and 93.8° , which are close to the p^3 bond angle (90°). These bond angles are in sharp contrast with the P films where the bond angles are rather large and are close to that of the sp^3 bond angle. The total density map in Fig. 6(a) shows that the p orbital mainly contributes to the chemical bonding charge. This charge density is in sharp contrast with that of the P black phosphorus crystal which has the component of the sp^3 dangling bond. As the DOS of this structure in Fig. 5 shows,

the film having this structure is metallic, i.e., the substantial DOS appears at the Fermi energy. The electron charge at the Fermi energy shows that the orbital mainly consists of the p orbital, due to the fact that the covalent bond type is p^3 .

In the most stable buckled structure, the two top atoms are inequivalent, so θ_2 defined in Fig.1 has two different values. The values of θ_2 of the top and the second atoms are 84.0° and 105.2° , respectively. while that of θ_1 is 93.8° . Therefore, the bond angle of the second top atom is rather large, indicating that the sp hybridization of the second top atom is enhanced. The values of l_1 and l_2 are 3.08\AA and 2.99\AA , respectively, so the bond lengths are enlarged in the buckled structure.

The electron charge of the valence top shown in Fig. 6(b) indicates that the surface chemical bond charge mainly consists of the sp^3 hybridized orbital of the second top and the component of the top atom is small. On the other hand, the charge distribution of the conduction band bottom mainly consists of the component of the top atom(Fig. 6(c)). Therefore we conclude that there is charge transfer from the top atom to the second top one and this charge transfer is the origin of the opening of the band gap.

The above mentioned charge transfer is due to the fact that the energy of the second atom orbital along the surface bond is lowered by buckling that makes the increases the bond angle of the second top atom (Since the increases of the bond angle enlarges the s component of the orbital, the orbital energy is lowered). This charge transfer found in the Bi film is in sharp contrast with that of the Si (001) surface having buckled dimers, i.e., the top (second top) atom forms sp^3 (sp^2) hybridization and thus the π electrons are transferred from the second top atom to the top one.¹⁵⁾

We finally discuss the difference between the P and Bi films. The P atom favors sp hybridization while Bi atom does p^3 bond. The inhibition of the sp hybridization of Bi is due to the fact that the s orbital is shrunked in the real space compared with the p orbital, so the contribution of the s component to the chemical bond is very small. It is known that as the element number becomes large, the contribution of the s orbital to the chemical bond decreases.¹⁶⁾ Since the P atom favors sp hybridization, the calculated bond angles of the P crystal and P nanofilms are rather close to the sp^3 bond angle(109.5°) as is seen from Table I. As a result, the charge contains sp^3 hybridized dangling bond (Fig.

2). Since this dangling bond is rather stable, the P film is not buckled.

On the other hand, since the Bi atom does not favor the sp hybridization, it tends to form p^3 bond without the s component. As a result, the nonbuckled two-layer film forms the bond angles of 93.8° and 95.8° , which are close to the p^3 bond angle (90°). Due to the buckling, the second top atom forms sp^3 bond angle and its atomic orbital energy is lowered since the s component increases. This is the reason why the buckled structure is more stable than the nonbuckled structure.

The electron transfer from the top atom to the second top atom induces inequivalent charge distribution which is similar to that in the case of the charge density wave (CDW). Since the nonbuckled and buckled structures have the same unit cell, however, the present system is not classified into the CDW system. In any case, the electron-lattice interaction is the origin of the buckling structure having the substantial gap.

Experimentally four-layer films are observed.¹⁰⁾ This film originates from stacking of the two two-layer films having the paired structure and the interaction between the two parts is weak. Our previous calculation indicated that the two surface atoms in the most stable structure are buckled and this film has DOS of semimetal.¹⁰⁾ This buckled structure is observed by an scanning tunneling microscopy (STM) experiment.¹⁰⁾ An STM image of the nonbuckled structure, which is metastable, may be observed under some experimental condition.

4. Summary

We performed first-principles calculations on P and Bi nanofilms. The band gap of the two-layer film of P is 1.2 eV and the value decreases and is expected to become close to that of crystal as the thickness becomes large. The two-layer Bi film has the most stable buckled structure with the band gap of 0.2 eV. On the other hand, the nonbuckled structure is metastable and metallic. The opening of the band gap in the buckled structure is found to be induced by the charge transfer from the top atom to the second one.

This work was supported by a Grant-in-Aid for Scientific Research (No. 17510097) from Japan Society for the Promotion of Science (JSPS). A part of this research was done in "Revolutionary Simulation Software for the 21st century" project supported

by Research and Development for Next-generation Information Technology of Ministry of Education, Culture, Sports, Science and Technology. The computation in this work has been done using the facilities of the Supercomputer Center, Institute for Solid State Physics, University of Tokyo.

References

- 1) R. M. Tromp, A.W. Denier van der Gon, F. K. LeGoues, and M. C. Reuter, *Phys. Rev. Lett.* 71 (1993) 3299.
- 2) E. Z. Luo, S. Heun, M. Kennedy, J. Wollschlaeger, and M. Henzler, *Phys. Rev. B* 49, 4858 (1994.); Yeh, and M. Tringides, *Phys. Rev. B* 61, (2000) R10602.
- 3) J. Tersoff and R. Tromp, *Phys. Rev. Lett.* 70 (1993) 2782.
- 4) B. J. Hinch, et al., *Europhys. Lett.* 10 (1989) 341.
- 5) L. Gavioli, K. R. Kimberlin, M. C. Tringides, J. F. Wendelken, and Z. Zhang, *Phys. Rev. Lett.* 82 (1999) 129.
- 6) I. Matsuda, H.W. Yeom, T. Tanikawa, K. Tono, T. Nagao, S. Hasegawa, and T. Ohta, *Phys. Rev. B* 63 (2001) 125325.
- 7) K. Budde, E. Abram, V. Yeh, and M. Tringides, *Phys. Rev. B* 61 (2000) R10602.
- 8) H. Hong et al., *Phys. Rev. Lett.* 90, 076104 (2003).
- 9) T. H. Cho, Q. Niu, and Z. Zhang, *Phys. Rev. Lett.* 82 (1999) 129 and references therein.
- 10) T. Nagao, J. T. Sadowski, M. Saito, S. Yaginuma, Y. Fujikawa, T. Kogure, T. Ohno, Y. Hasegawa, S. Hasegawa, and T. Sakurai, *Phys. Rev. Lett.* , 93, (2004) 105501.
- 11) M. Saito, T. Ohno, and T. Miyazaki, *Appl. Surf. Sci.* 237 (2004) 80.
- 12) J. T. Sadowski, T. Nagao, S. Yaginuma, Y. Fujikawa, A. Al-Mahboob, G. E. Thayer, R. M. Tromp, *Appl. Phys. Lett.* 86,073109 (2005).
- 13) A. Brown and S. Rundquist, *Acta Cryst.* 19, 684 (1965).
- 14) R. W. Keyes, *Phys. Rev.* 92, 580 (1953); D. Warschauer, *J. Appl. Phys.* 34, 1853 (1963).
- 15) J. Ihm, M. L. Cohen, D.J.Chadi, *Phys. Rev.*, B21, 4592 (1980).
- 16) Z. Tang, M. Hasegawa, T. Chiba, M. Saito, H. Sumiya, Y. Kawazoe, and S. Yamaguchi, *Phys. Rev. B* 57, 12219 (1998).

Table I. Table I. Crystal parameters of P crystal and P nanofilms. The values in parentheses are experimental ones. The unit of the lengths of a , b , c , l_1 and l_2 are Å.

	a	b	c	l_1	l_2	θ_1	θ_2
crystal	4.40	11.21	3.40	2.27	2.29	97.2	103.7
	(4.37)	(10.48)	(3.31)	(2.22)	(2.24)	(96.3)	(102.1)
2-layer film	4.64		3.37	2.26	2.32	96.4	103.5
4-layer film	4.61		3.38	2.26	2.29	96.6	103.4
6-layer film	4.60		3.38	2.26	2.29	96.9	103.4

Figure captions

Fig. 1. The unit cell of the P crystal indicated by the rectangular parallelepiped.

Fig. 2. Total electron charges of the P crystal (a) and the two-layer P film (b).

Fig. 3. The DOS of P films. The DOS of the two-layer (a), four-layer (b), and six-layer (c) films are shown. The energy is measured from the valence band top.

Fig. 4. Stable (a) and (b) metastable atomic structures of Bi two-layer films.

Fig. 5. DOS of the Bi two-layer film having the stable (a) and metastable (b) structures. The energy is measured from the valence band top (a) and the Fermi energy (b).

Fig. 6. Partial electron charge at the Fermi energy of the metastable structure (a) and those of the valence band top (b) and conduction band bottom (c) of the stable structure.

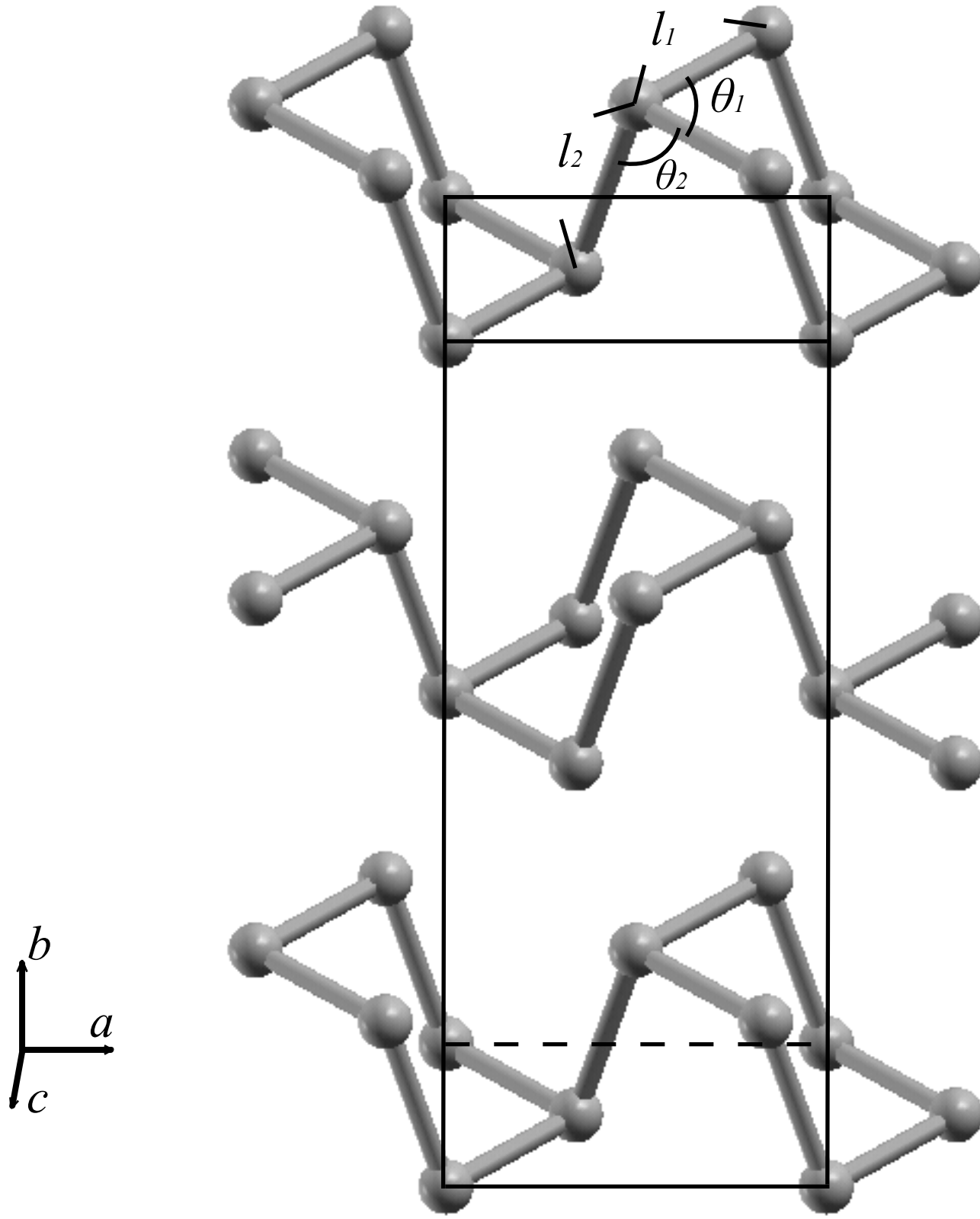


Fig.1

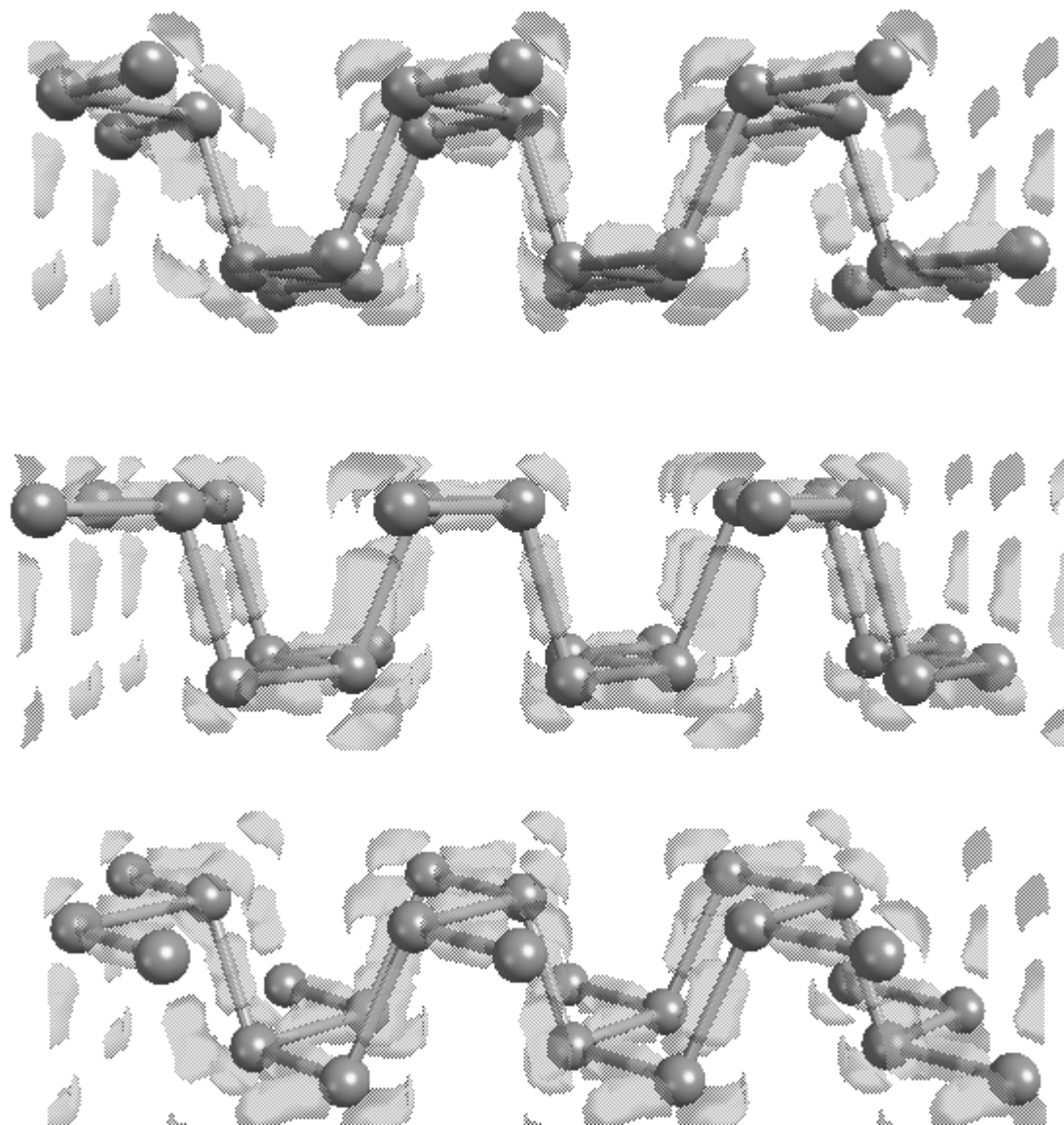


Fig.2(a)

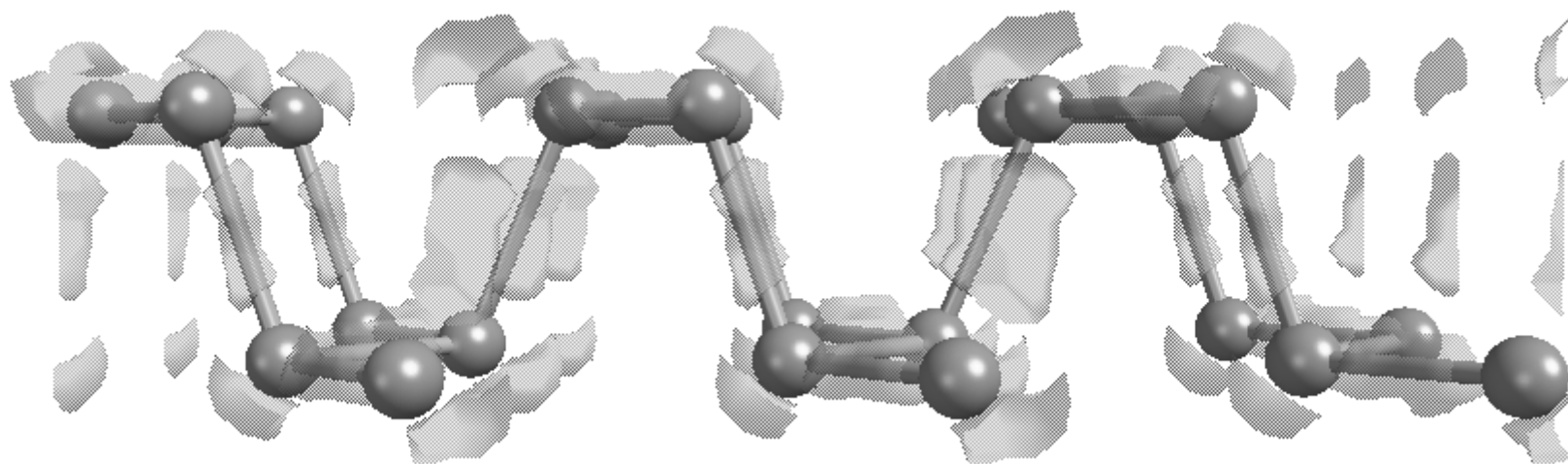


Fig.2(b)

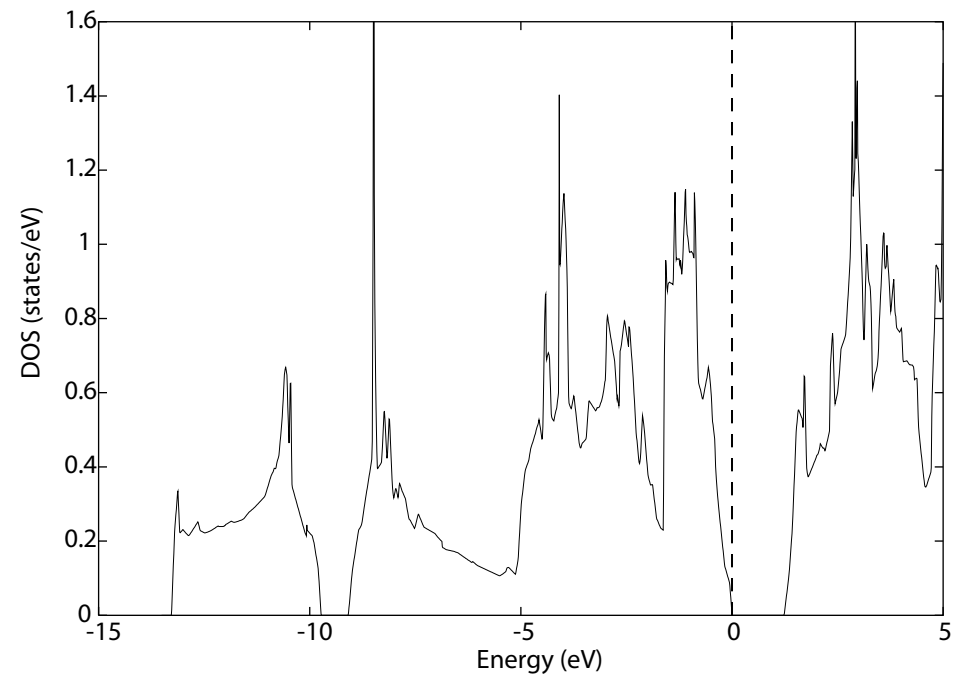


Fig.3(a)

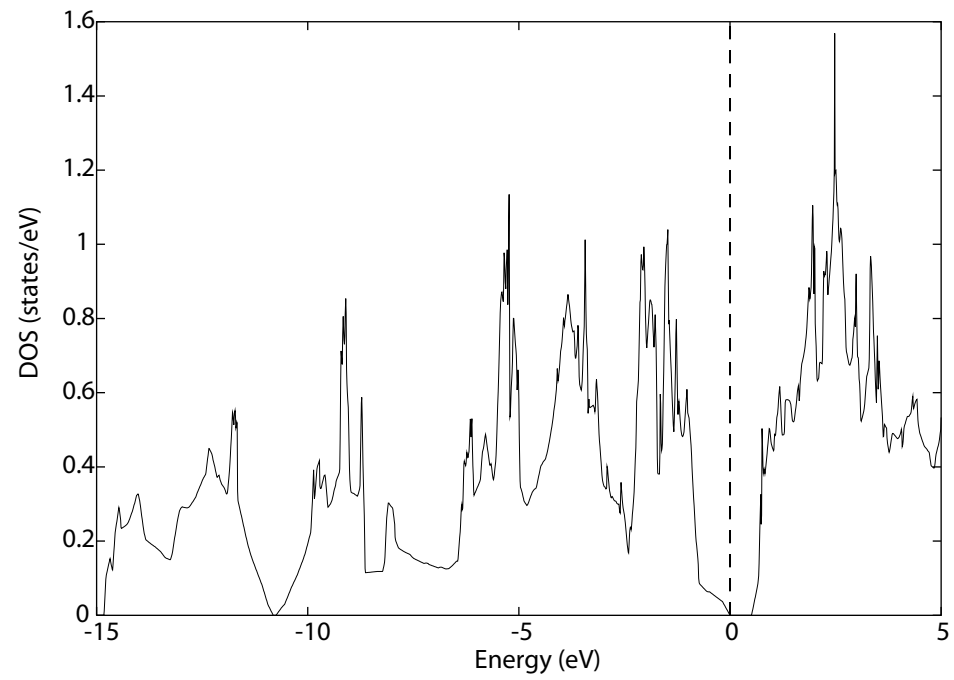


Fig.3(b)

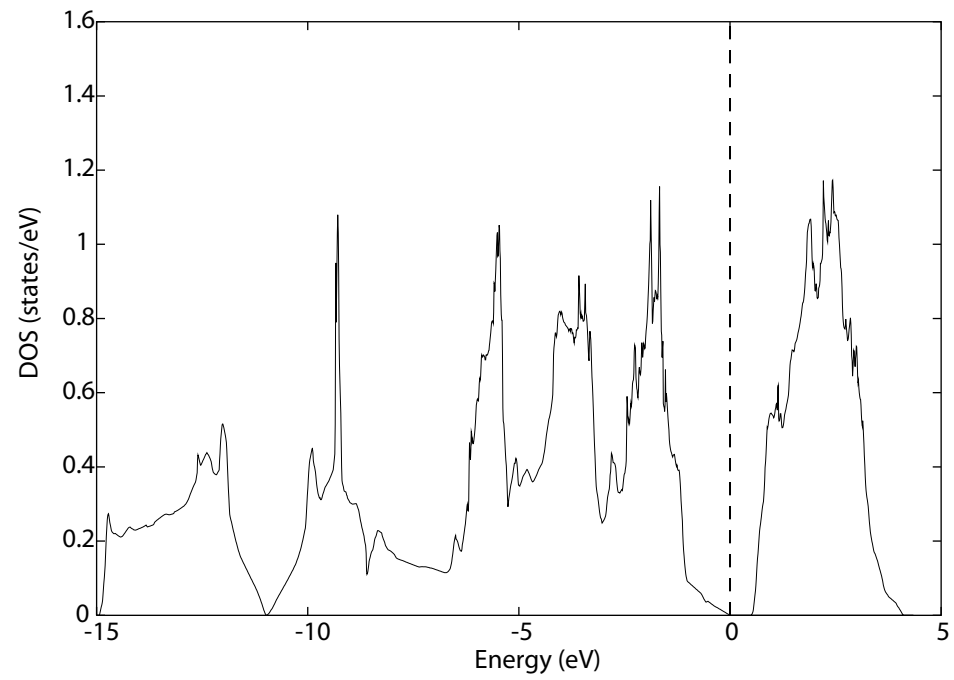


Fig.3(c)

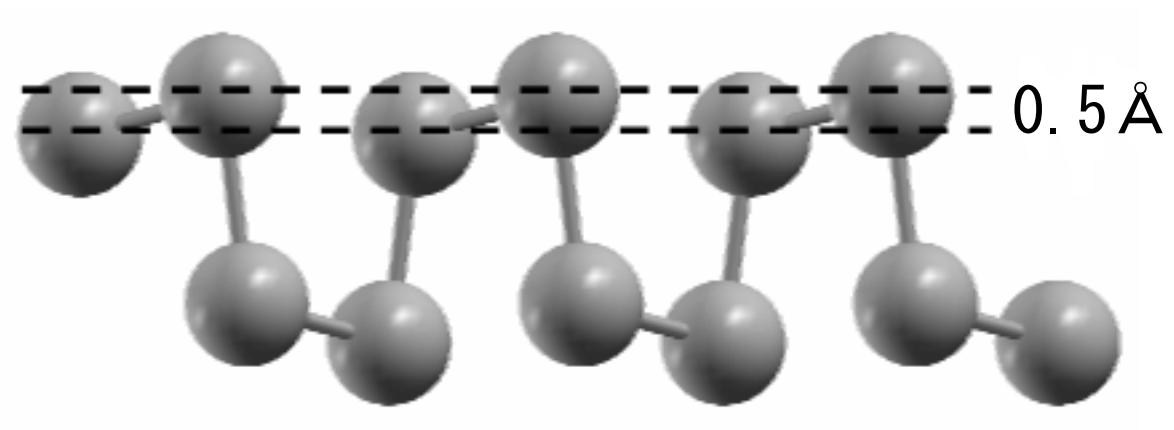


Fig4.(a)

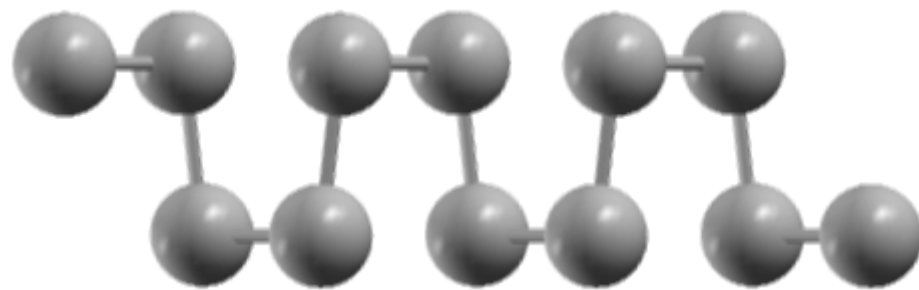


Fig4.(b)

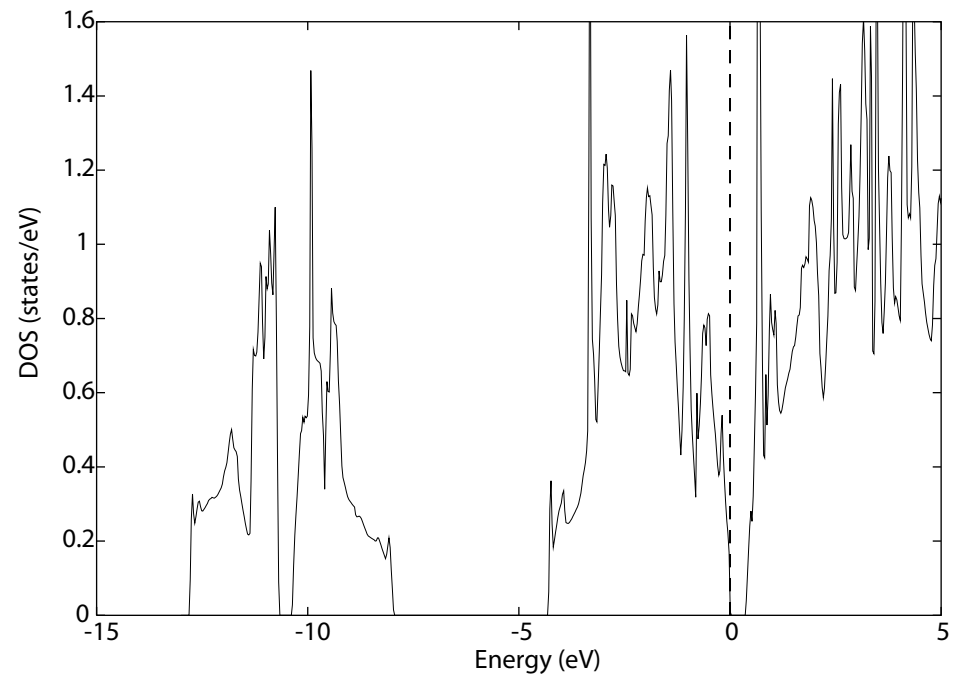


Fig5.(a)

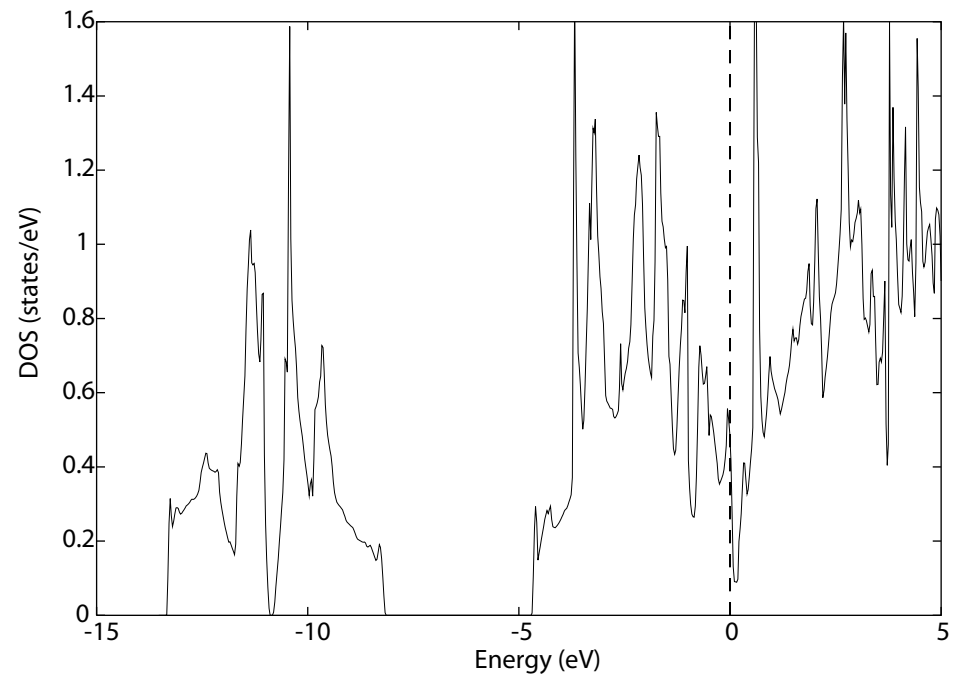


Fig5.(b)

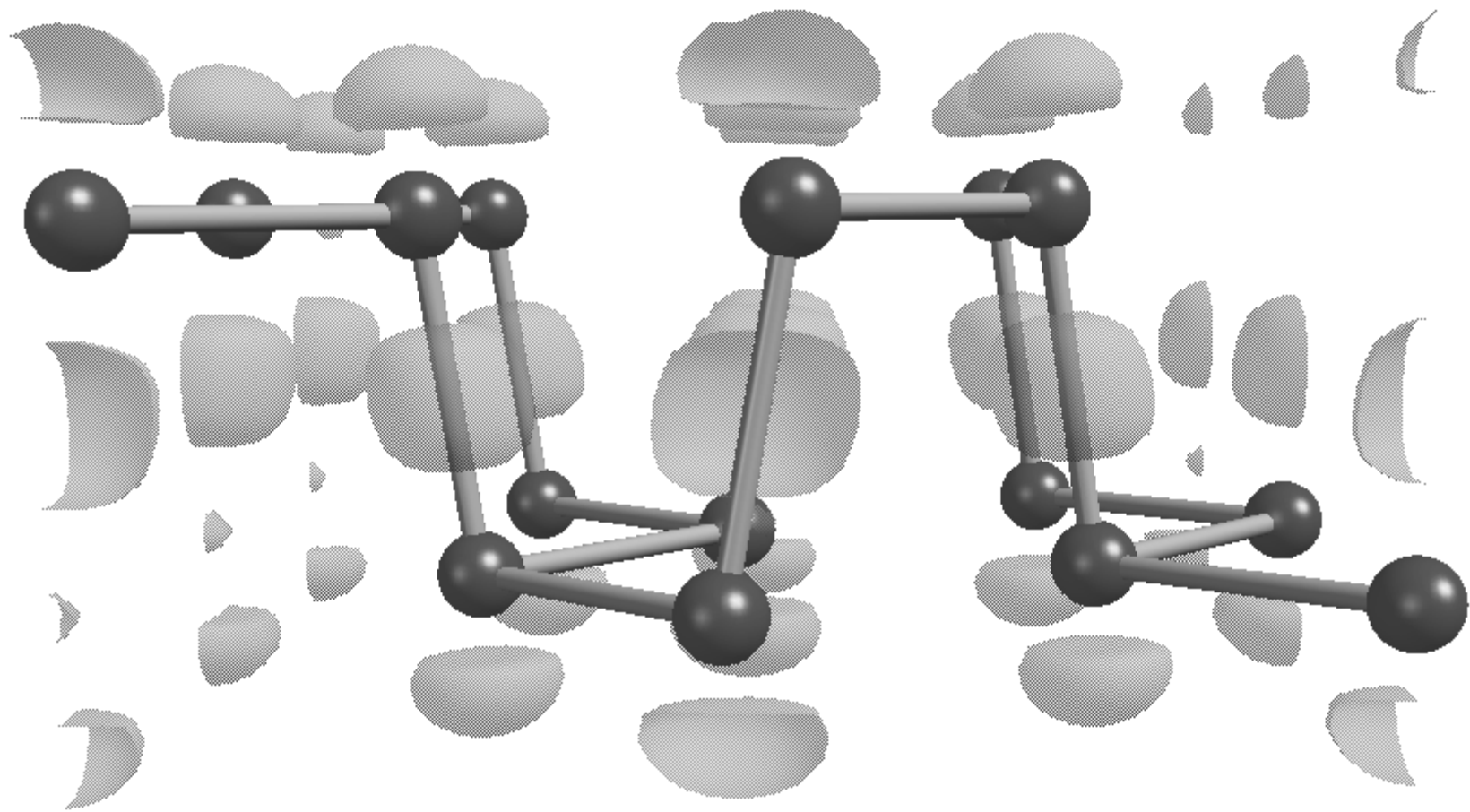


Fig6.(a)

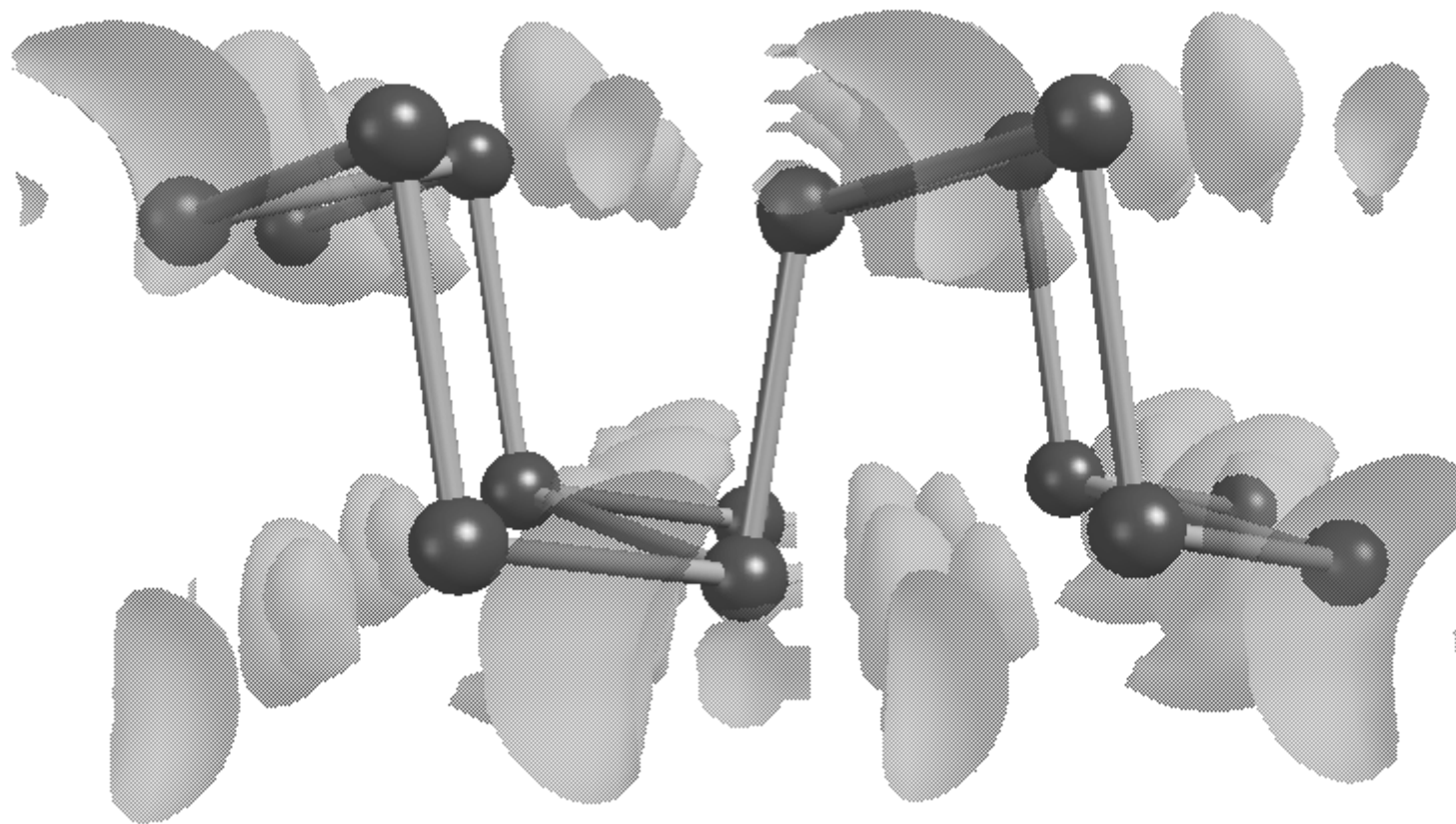


Fig6.(b)

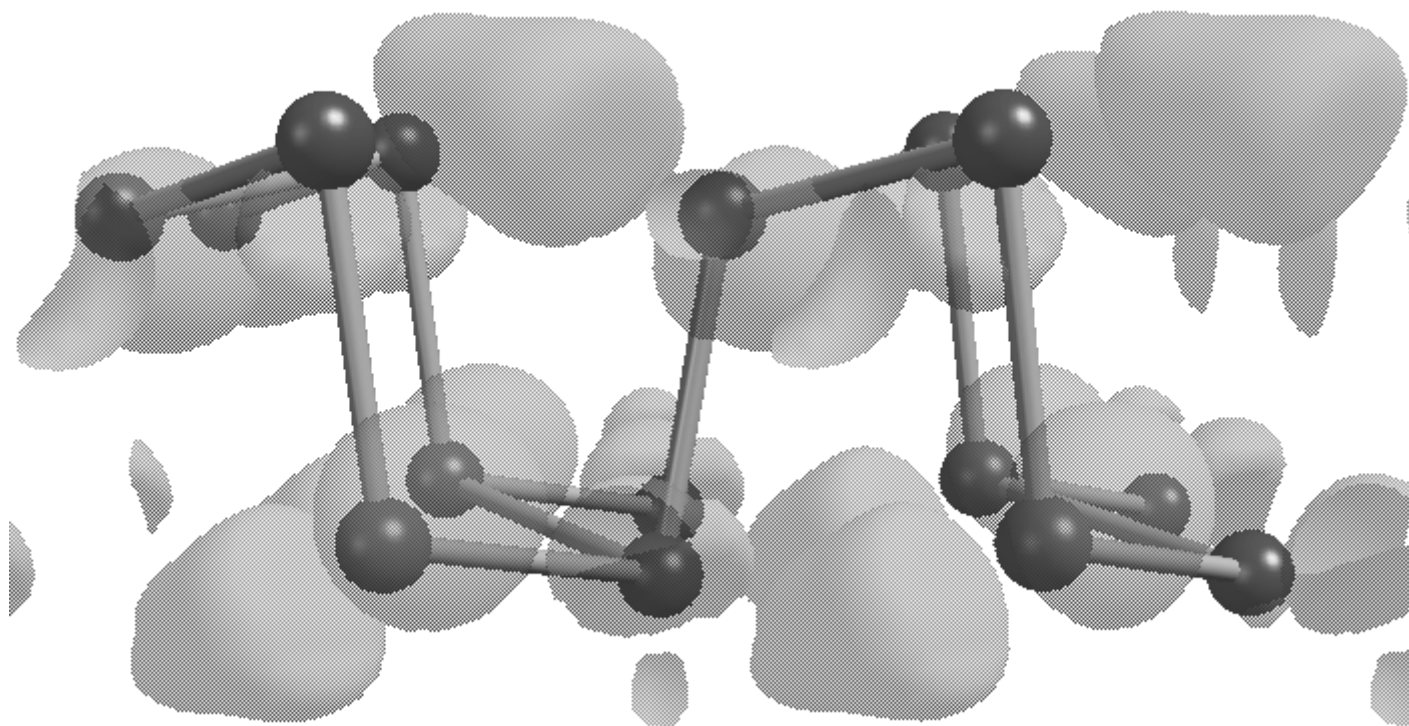


Fig6.(c)